Journal of Alloys and Compounds 505 (2010) 754–757

Contents lists available at ScienceDirect

Journal of Alloys and Compounds

journal homepage: www.elsevier.com/locate/jallcom

Structural and physical characteristics of CeO_2–GeO_2–PbO glasses and glass ceramics

Eugen Culea, Lidia Pop*, Maria Bosca

Technical University of Cluj-Napoca, C. Daicoviciu 15, 400020 Cluj-Napoca, Romania

ARTICLE INFO

Article history:
Received 8 February 2010
Received in revised form 21 June 2010
Accepted 22 June 2010
Available online 1 July 2010

Keywords:
Disordered systems
XRD
FT-IR Spectroscopy
Magnetic measurements

ABSTRACT

Samples of the $x$$CeO_2$(100 − x)[GeO_2·PbO] system with $0 \le x \le 15$ mol% were prepared and characterized by X-ray diffraction, FT-IR spectroscopy and magnetic measurements. The X-ray diffraction (XRD) investigation revealed the presence of a crystalline phase for samples with $x \ge 3$ mol%, namely that of $Ce_{1.88}Pb_{2.12}O_{6.53}$. The structural role of germanium, lead and cerium ions was discussed. The presence of the CeO_4, GeO_4, GeO_6 and PbO_4 structural units was evidenced by FT-IR spectrocopy in the studied glasses and glass ceramics. It was shown that the ratio of the mentioned structural units depends on the CeO_2 content of the $x$$CeO_2$(100 − x)[GeO_2·PbO] system. As a part of an on-going investigation of the physical properties of $x$$CeO_2$(100 − x)[$GeO_2$·PbO] glass ceramics, the magnetic behavior of this system was studied. The fractions of the cerium ions in the 3+ and 4+ valence states were determined.

1. Introduction

Recently multicomponent glasses have received much attention as materials which offer various applications in optics and optoelectronics. It is known that, in general, the oxide glasses possess a good mechanical strength, chemical durability and thermal stability [1–3]. Among the different vitreous systems studied earlier, the PbO–GeO_2 glasses are technologically important because of their potential use as low loss optical glasses in the infrared region [4–6]. Moreover the study of lead–germanate glasses is of particular interest since they can be easily obtained into fiber form for their use in optoelectronics. These glasses are also suitable for waveguide applications. The lead–germanate glasses show important properties such as a good chemical durability and mechanical stability, a higher glass transition temperature and, as a consequence, higher laser damage thresholds at 3 μm [7,8].

On the other hand, glasses and crystals containing rare-earths have attracted great attention because of their extensive applications in fields such as information display, advanced laser materials and fiber optical communication [9–11]. It is worth mentioning that Ce, as well as other rare-earth and transition metal ions in glasses, exists in multivalent states which give rise to the interesting magnetic and semiconducting behavior of the host glasses (i.e. [12–18]).

In order to obtain more information concerning the important class of lead–germanate glasses doped with rare-earth ions, in the present paper we studied some structural and magnetic properties of the $x$$CeO_2$(100 − x)[GeO_2·PbO] system with $0 \le x \le 15$ mol%. The effect of the progressive addition of CeO_2 on the structural and physical properties of the GeO_2·PbO host matrix was followed by means of X-ray diffraction, FT-IR spectroscopy and magnetic susceptibility measurements.

2. Experimental

Samples of the cerium–lead–germanate system having the general formula $x$$CeO_2$(100 − x)[GeO_2·PbO] where x = 0, 1, 3, 5, 7, 10, 15 mol% were prepared by the melt quenching method. Required quantities of analar grade GeO_2, PbO and CeO_2 were mixed and miled together with the aim to obtain a fine powder. The mixture was melted in sintered corundum crucibles in an electric furnance at a temperature of 1100 °C for 15 min. The samples were obtained by pressing the melts between two steal plates.

The samples were studied by X-ray diffraction using a XRD-6000 SHIMADZU diffractometer. The Cu Kα radiation (λ = 1.54056 Å), a working voltage of 40 kV, a working current of 30 mA and the scanning speed of 2°/min were used.

The FT-IR investigation was performed using a JASCO FT-IR 6200 spectrometer. The FT-IR spectra were recorded at room temperature, using the KBr pellet technique in the 400–1700 cm^{-1} range. In order to obtain good quality spectra the samples were crushed in an agate mortar to obtain a fine powder.

The magnetic susceptibility measurements were performed using a Faraday-type balance in the 80–300 K temperature range. The diamagnetic susceptibility of the GeO_2·PbO base glass was measured, too, and the magnetic susceptibility data for all the samples were corrected taking into account the diamagnetic contribution of the host matrix.

* Corresponding author. Tel.: +40 264 401 262; fax: +40 264 595 355.
E-mail address: Lidia.Pop@phys.utcluj.ro (L. Pop).

0925-8388/$ – see front matter © 2010 Elsevier B.V. All rights reserved.
doi:10.1016/j.jallcom.2010.06.135

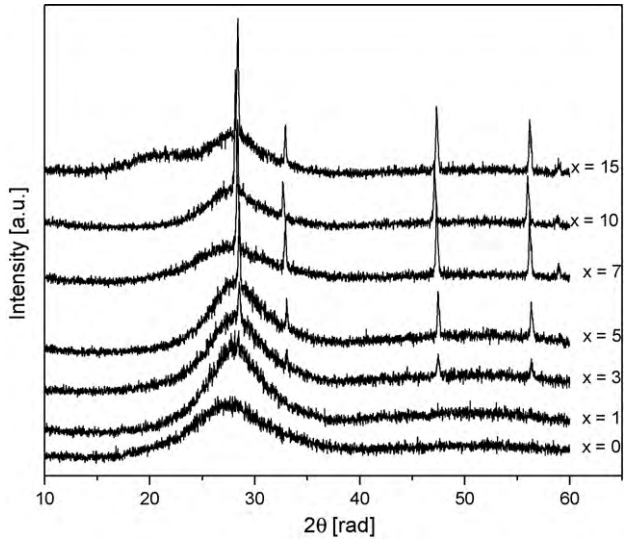

Fig. 1. X-ray diffraction patterns for the xCeO$_2$(100 − x)[GeO$_2$·PbO] system.

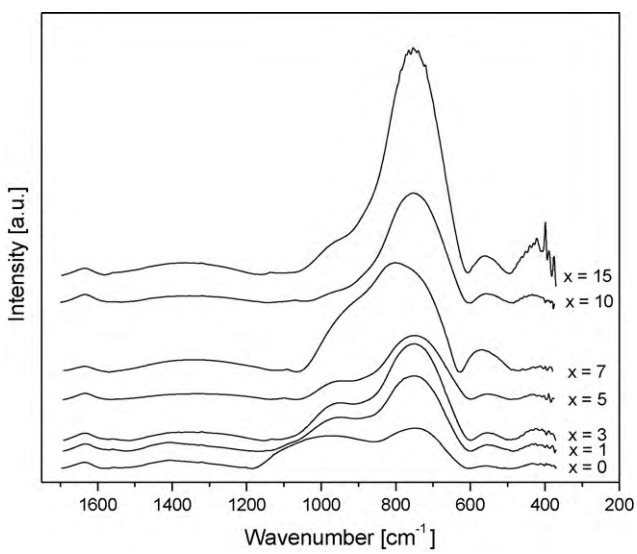

Fig. 2. FT-IR spectra of the xCeO$_2$(100 − x)[GeO$_2$·PbO] system.

3. Results and discussion

The X-ray diffraction patterns of the samples from the xCeO$_2$(100 − x)[GeO$_2$·PbO] system are shown in Fig. 1. The diffractograms for the samples with $x \leq 1$ mol% show the broad diffuse scattering characteristic of amorphous structure. For the samples with $x \geq 3$ mol% the diffractograms present a superposition of the broad diffuse scattering characteristic of amorphous structure with some peaks characteristic of crystalline phases. In order to identify the crystalline phases that appear in the diffraction patterns we followed a standard procedure, namely the computer analysis based on the powder diffraction file (PDF). This analysis permitted the identification of the crystalline phase present in the samples which was determined to be the $Ce_{1.88}Pb_{2.12}O_{6.53}$ one (PDF nr. 48-0059, face centered cubic lattice with the $\alpha = 5.417$ cell parameter). The assignments and relative intensities (I) of the four most important crystalline peaks are: $2\theta = 28.583$ rad with $I = 100$ ($h = 1$, $k = 1$, $l = 1$), $2\theta = 33.049$ rad with $I = 39$ ($h = 2$, $k = 0$, $l = 0$), $2\theta = 47.433$ rad with $I = 57$ ($h = 2$, $k = 2$, $l = 0$) and $2\theta = 56.270$ rad with $I = 50$ ($h = 3$, $k = 1$, $l = 1$).

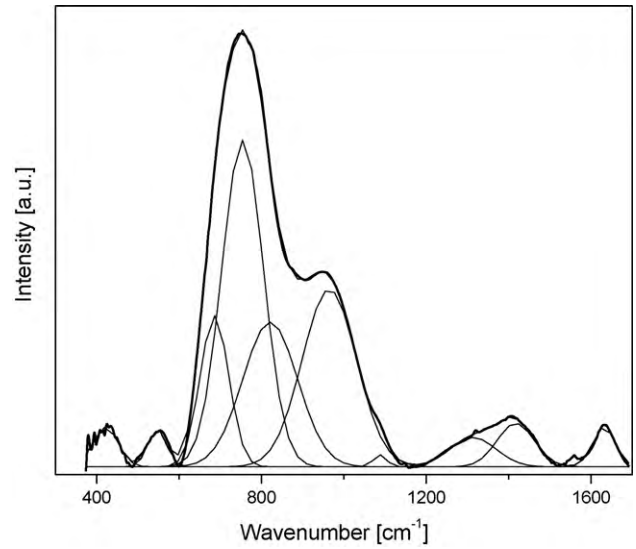

Fig. 3. The result of the deconvolution of the FT-IR spectrum for the 1CeO$_2$·99[GeO$_2$·PbO] sample.

Vibrational FT-IR spectra of the xCeO$_2$(100 − x)[GeO$_2$·PbO] samples with $x = 0$, 1, 3, 5, 7, 10, 15 mol% are shown in Fig. 2. Since most of the IR bands present in these spectra are very broad and asymmetric due to the amorphous (or partly amorphous) nature of the samples, a deconvolution procedure of the experimental spectra was necessary. This procedure was performed with the Spectra Manager program using a Gaussian type function. Fig. 3 shows the deconvolution, in Gaussian bands, of the spectrum for the 1CeO$_2$·99[GeO$_2$·PbO] sample. The deconvolution procedure allowed us a better identification of the IR bands that appear in the experimental spectra, offered the possibility to calculate their relative area and thus to follow more precisely their compositional evolution. Each component IR absorption band is related to some type of vibration in specific structural groups. The positions of the most important absorption bands evidenced in the FT-IR spectra and their assignments are summarized in Table 1. The assignments

Table 1
FT-IR bands and there assignments for the xCeO$_2$(100 − x)[GeO$_2$·PbO] samples.

Wavenumber [cm^{-1}]	Assignments
425	Symmetric bending vibration mode of Pb–O in PbO$_4$ units [25,26] bending vibration mode of Ce–O in CeO$_4$ units [27]
555	Symmetric stretching mode of Ge–O–Ge bonds [19,22,23] asymmetric bending vibration modes of Pb–O–Pb bonds [25]
690	Stretching mode of Ge–O–Ge bonds in GeO$_6$ units [21,24,27]
760	Asymmetric stretching mode of Ge–O–Ge bridges connecting GeO$_4$ units [22,23]
870	Asymmetric stretching mode of Ge–O–Ge bonds from GeO$_4$ units [19,22,27]
965	Symmetric stretching vibration modes of Pb–O bonds [25,26]
1130	Asymmetric stretching vibration modes of Pb–O bonds [25]
1320	Bending vibration mode of Pb–O–Ge bonds
1430	Asymmetric stretching vibration modes of Ge–O–Ge bonds [19]
1635	OH bending mode of vibration

Table 2
Compositional variation of the magnetic parameters of the $xCeO_2(100-x)[GeO_2{\cdot}PbO]$ samples.

x [mol%]	$-\theta_p$ [K]	C_M [uem/mol]	μ_{eff} [μ_B/atom]
3	0	0.01275	1.84
5	3	0.02014	1.8
7	6	0.02814	1.79
10	10	0.03808	1.74
15	12	0.05744	1.75

were made based on data from the literature concerning some related vitreous or crystalline compounds [19–29].

The comparison of the FT-IR spectrum of the $[GeO_2{\cdot}PbO]$ host matrix with the spectra obtained for the samples doped with cerium oxide reveals remarkable structural changes produced as a consequence of the addition of cerium ions (Table 2).

It was shown that GeO_2 appears in the glass networks as GeO_4 structural units (with the Ge–O bonds of 1.739 ± 0.002 Å) or both GeO_4 and GeO_6 units (where four Ge–O bonds are of 1.827 Å, while the other two are of 1.902 Å) [30]. The most important FT-IR feature showing the presence of the GeO_6 units in the samples is the absorption band around 690 cm^{-1} [21,24,27]. The analysis of the FT-IR spectra from Fig. 2 shows that the Ge^{4+} cations are incorporated in the studied $xCeO_2(100-x)[GeO_2{\cdot}PbO]$ system as GeO_4 and GeO_6 units. On the other hand, PbO may also participate in the glass network with PbO_4 structural units when the lead ion is linked to four oxygens in a covalency bond configuration as mentioned earlier [31].

With the increase of the concentration of CeO_2 into the glass network, the shape of the FT-IR spectra is affected by the presence of the crystalline phase evidenced by the XRD measurement. Thus, the absorption bands from 690 and 760 cm^{-1} become more intense and narrow for higher contents of cerium oxide. At the same time, the bands from 870 and 965 cm^{-1} decrease in intensity for higher contents of cerium oxide. These observations indicate two important changes produces by increasing the CeO_2 concentration of the samples: (i) a gradual conversion of the GeO_4 units into the more stable GeO_6 units and (ii) a decrease of the symmetric stretching vibration modes of Pb–O bonds (suggesting the depolymerization of the vitreous matrix). These structural changes are in agreement with the increase of the structural order of the samples determined by increasing their CeO_2 content, namely the appearance of the $Ce_{1.88}Pb_{2.12}O_{6.53}$ crystalline phase, as revealed by the XRD data.

The presented data indicate the fact that the addition of CeO_2 to the host $GeO_2{\cdot}PbO$ matrix produces major structural modifications. The structural changes observed by the FT-IR investigation suggest that the cerium ions play a network modifier role in the studied $xCeO_2(100-x)[GeO_2{\cdot}PbO]$ system while germanium and lead ions play the network former role.

Fig. 4 presents the dependence of the inverse magnetic susceptibility as function of temperature for the $xCeO_2(100-x)[GeO_2{\cdot}PbO]$ samples.

Since the magnetic susceptibility data shown that the germanium–lead host glass matrix was diamagnetic, the magnetic behavior of the studied glasses and glass ceramics was assumed to be due to the presence of the cerium ions in the samples. The cerium ions may be present in glasses in both the 3+ and 4+ valence states [i.e., 29]. The Ce^{3+} ions (due to their $4f^1$ electronic configuration) are magnetic species with a magnetic moment of 2.56 μB [29], while the Ce^{4+} ions (with no unpaired electronic spin – $4f^0$ electronic configuration) are diamagnetic [32]. Thus, only the Ce^{3+} ions will determine the magnetic behavior of the studied $xCeO_2(1-x)[GeO_2{\cdot}PbO]$ samples.

By fitting the experimental magnetic susceptibility data, we determined the values of important magnetic parameters: the paramagnetic Curie temperatures, the Curie constants and the effective magnetic moments per cerium 3+ ions. The magnetic susceptibility data were corrected taking into account the diamagnetic contribution of the germanium–lead host glass matrix.

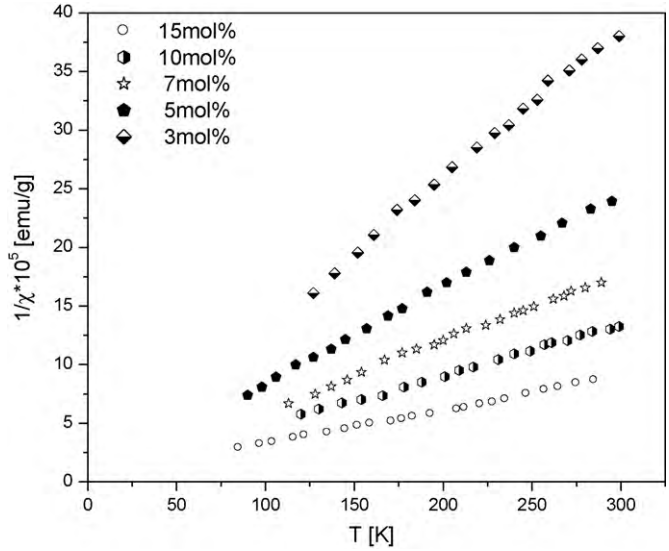

Fig. 4. Thermal variation of the reciprocal magnetic susceptibility for $xCeO_2(100-x)[GeO_2{\cdot}PbO]$ system.

Fig. 5 presents the compositional evolution of the paramagnetic Curie temperature, θ_p, for the $xCeO_2(100-x)[GeO_2{\cdot}PbO]$ system. The paramagnetic Curie temperature is a rough indicator of magnetic interaction between the magnetic cerium ions. The negative values of θ_p suggest the presence of antiferromagnetic interactions between the cerium ions. Thus, for the samples with $x \geq 3$ mol%, the magnetic Ce^{3+} ions will appear not only as isolated species but also as coupled species, namely the Ce^{3+}–O–Ce^{3+} species coupled via superexchange interactions.

The compositional dependence of the paramagnetic Curie temperatures (Fig. 5) show a Curie-type behavior for the samples with low cerium oxide contents ($x < 3$ mol%) and a Curie–Weiss behavior for he samples with higher cerium oxide contents ($x \geq 3$ mol%).

Using the assumed value of 2.56 μ_B for the effective magnetic moment of the Ce^{3+} ions [24], the fraction of Ce^{3+} ions was esti-

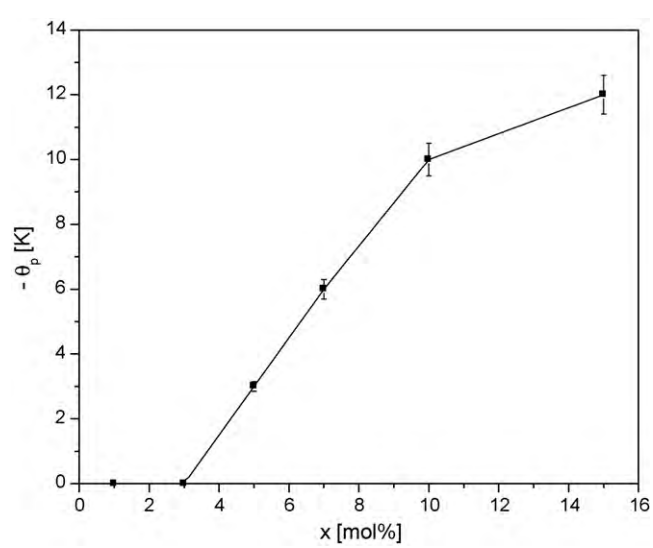

Fig. 5. The composition dependence of the paramagnetic Curie temperature of $xCeO_2(100-x)[GeO_2{\cdot}PbO]$ glass ceramics system (the line is only a guide for the eye).

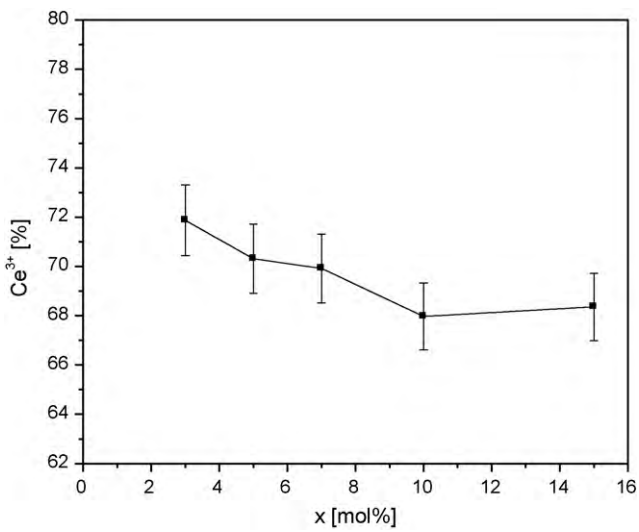

Fig. 6. The composition dependence of the fraction of Ce^{3+} ions (the line is only a guide for the eye).

mated. The composition dependence of the fraction of cerium ions in 3+ valence state is plotted in Fig. 6.

4. Conclusions

The structure and properties of $x CeO_2(100-x)[GeO_2 \cdot PbO]$ glasses and glass ceramics with $0 \le x \le 15$ mol%, prepared by the melt quenching method, have been investigated. The investigation of the mentioned system permitted to obtain some important information, as follows:

(i) The XRD data indicate that the addition of CeO_2 to the $GeO_2 \cdot PbO$ host glass matrix over $x = 3$ mol% generates the appearance of the $Ce_{1.88}Pb_{2.12}O_{6.53}$ crystalline phases.
(ii) The FT-IR spectra show that the cerium ions act as network modifiers in the host matrix, while germanium and lead ions play the network former role. The cerium ions are present in the studied samples in the CeO_4 structural units. The germanium and lead ions are presents in the $x CeO_2(100-x)[GeO_2 \cdot PbO]$ system in the GeO_4, GeO_6 and PbO_4 structural units. The number of GeO_6 and PbO_4 structural units increases with the addition of cerium oxide.
(iii) Magnetic susceptibility data evidenced that cerium ions are present in both their 3+ and 4+ valence state but the 3+ state is predominant. With increasing the cerium oxide content of the samples the number of the 4+ cerium ions increases.
(iv) Magnetic interactions between the Ce^{3+} ions are of antiferromagnetic nature.

Acknowledgement

The financial support of the Ministry of Education and Research of Romania-National University Research Council (CNCSIS, PN II-IDEI 183/2008, contract number 476/2009) is gratefully acknowledged by the authors.

References

[1] G. Dominiak-Dzik, W. Ryba-Romanowski, J. Alloys Compd. 451 (2008) 586–590.
[2] L.S. Du, L. Peng, J.F. Stebbins, J. Non-Cryst. Solids 353 (2007) 2910–2918.
[3] L. Pop, E. Culea, M. Bosca, R. Muntean, M. Culea, J. Optoelect. Adv. Mater. 9 (2007) 561–563.
[4] N. Sooraj Hussain, Y. Prabhakara Reddy, S. Buddhudu, Mater. Lett. 53 (2002) 25–29.
[5] D.M. Shi, Y.G. Zhao, Q. Qian, D.D. Chen, Q.Y. Zhang, J. Alloys Compd. 499 (2010) 126–130.
[6] D.M. Shi, Q.Y. Zhang, G.F. Yang, C. Zhao, Z.M. Yang, Z.H. Jiang, J. Alloys Compd. 466 (2008) 373–376.
[7] D. Munoz-Martin, J. Gonzalo, J.M. Fernandez-Navarro, J. Siegel, C.N. Afonso, Appl. Surf. Sci. 254 (2007) 1111–1114.
[8] L.R.P. Kassab, W.G. Hora, J.R. Martinelli, F.F. Sene, J. Jakutis, N.U. Wetter, J. Non-Cryst. Solids 352 (2006) 3530–3534.
[9] H. Lin, W. Qin, J. Zhang, C. Wu, Solid State Commun. 141 (2007) 436–439.
[10] S. Rada, E. Culea, J. Mol. Struct. 929 (2009) 141–148.
[11] G. Lakshminarayana, J. Qiu, J. Alloys Compd. 476 (2009) 720–727.
[12] S. Hazra, A. Ghosh, Phys. Rev. B 51 (1995) 851–856.
[13] J. Wang, W. Chen, L. Luo, J. Alloys Compd. 464 (2008) 440–445.
[14] S. Sen, A. Ghosh, J. Phys.: Condens. Matter 11 (1999) 1529–1536.
[15] S. Mandal, A. Ghosh, Phys. Rev. B 49 (1994) 3131–3135.
[16] S. Mandal, A. Ghosh, Phys. Rev. B 48 (1993) 9388–9393.
[17] A. Ghosh, B.K. Chaudhuri, J. Non-Cryst. Solids 83 (1986) 151–161.
[18] A. Ghosh, J. Phys.: Condens. Matter 1 (1989) 7819–7828.
[19] N. Terakado, K. Tanaka, J. Non-Cryst. Solids 354 (2008) 1992–1999.
[20] L.M. Sharaf El-Deen, M.S. Al Salhi, M.M. Elkholy, J. Alloys Compd. 465 (2008) 333–339.
[21] P. Pascuta, E. Culea, Mater. Lett. 62 (2008) 4127–4129.
[22] Y. Kim, J. Saienga, S.W. Martin, J. Non-Cryst. Solids 351 (2005) 3716–3724.
[23] L.F. Santos, L. Wondraczek, J. Deubener, R.M. Almeida, J. Non-Cryst. Solids 353 (2007) 1875–1881.
[24] S. Simon, I. Ardelean, S. Filip, I. Bratu, I. Cosma, Solid State Commun. 116 (2000) 83–86.
[25] G.L.J. Trettenhahn, G.E. Nauer, A. Neckel, Vibrat. Spectrosc. 5 (1993) 85–100.
[26] M. Bosca, L. Pop, G. Borodi, P. Pascuta, E. Culea, J. Alloys Compd. 479 (2009) 579–582.
[27] M. Ferraris, D. Milanese, C. Contardi, Q. Chen, Y. Menke, J. Non-Cryst. Solids 347 (2004) 246–253.
[28] S.J.L. Ribeiro, O.L. Malta, G.F. de Sá, J. Dexpert-Ghys, B. Piriou, H. Dexpert, V.R. Mastelaro, J. Alloys Compd. 180 (1992) 117–124.
[29] E. Burzo, I. Ardelean, D. Matulescu, J. Mater. Sci. Lett. 11 (1992) 1496–1497.
[30] A. Witkowska, B. Sikora, K. Trzebiatowski, J. Rybicki, J. Non-Cryst. Solids 352 (2006) 4356–4361.
[31] P. Syam Prasad, B.V. Raghavaiah, R. Balaji Rao, C. Laxmikanth, N. Veeraiah, Solid State Commun. 132 (2004) 235–240.
[32] A. Normany, V. Perrichon, Phys. Chem. Chem. Phys. 5 (2003) 3557–3564.